

CREEP OF LITHIUM FLUORIDE SINGLE CRYSTALS  
AT ELEVATED TEMPERATURES

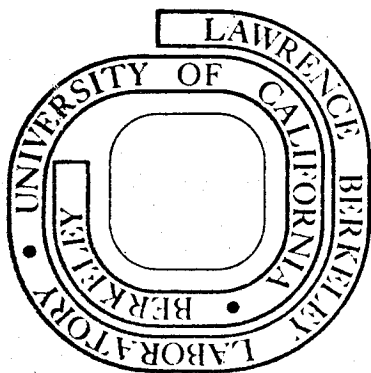
Donald R. Cropper and Joseph A. Pask

September 1972

Prepared for the U. S. Atomic Energy Commission  
under Contract W-7405-ENG-48

**For Reference**

Not to be taken from this room



## **DISCLAIMER**

This document was prepared as an account of work sponsored by the United States Government. While this document is believed to contain correct information, neither the United States Government nor any agency thereof, nor the Regents of the University of California, nor any of their employees, makes any warranty, express or implied, or assumes any legal responsibility for the accuracy, completeness, or usefulness of any information, apparatus, product, or process disclosed, or represents that its use would not infringe privately owned rights. Reference herein to any specific commercial product, process, or service by its trade name, trademark, manufacturer, or otherwise, does not necessarily constitute or imply its endorsement, recommendation, or favoring by the United States Government or any agency thereof, or the Regents of the University of California. The views and opinions of authors expressed herein do not necessarily state or reflect those of the United States Government or any agency thereof or the Regents of the University of California.

CREEP OF LITHIUM FLUORIDE SINGLE CRYSTALS  
AT ELEVATED TEMPERATURES\*

Donald R. Cropper and Joseph A. Pask

Inorganic Materials Research Division, Lawrence Berkeley Laboratory,  
and Department of Materials Science and Engineering,  
College of Engineering, University of California,  
Berkeley, California

ABSTRACT

The creep deformation of lithium fluoride single crystals was studied in compression over the temperature range 650°-750°C (0.8-0.9  $T_m$ ). Extended primary creep was observed for crystals deformed with the compression axis in  $\langle 100 \rangle$  orientation; strains of 0.20 or more were required for the establishment of steady-state conditions. Crystals with compression axes in the  $\langle 111 \rangle$  direction reached steady-state quickly, at strains of 0.05 or less. The steady-state strain rate was found to be proportional to the stress raised to the power  $n$ , where  $n$  ranged from 3.1 for  $\langle 111 \rangle$  crystals to 4.1 for  $\langle 100 \rangle$  crystals. The activation energy for creep was determined to be  $53 \pm 7$  kcal/mole over the temperature range considered, regardless of crystal orientation or impurity content up to 300 ppm total impurities; this compares favorably with the activation energy for lattice diffusion of the fluorine ion in LiF. Well developed substructures were observed in the deformed crystals with the subgrain diameter varying inversely with the applied stress. These results suggest that the creep deformation of lithium fluoride single crystals may be similar to that for metals and is probably dependent upon the dislocation climb process.

---

\*Based on thesis submitted by Donald R. Cropper in Jan. 1971 in partial fulfillment of the requirements for the Ph.D. degree in Ceramic Science.

## 1. INTRODUCTION

While the mechanical behavior of ionic crystals has been the subject of intensive study during recent years, there is surprisingly little information in the literature on the high temperature creep behavior of such materials.

Most studies of creep deformation are confined to measurements made under "steady state" or secondary creep conditions. Here the observed rate of deformation may be envisioned as a balance between the work hardening induced by continued deformation and the recovery processes operative at high temperatures.

The various theoretical models describing steady-state creep were recently reviewed by Mukherjee, Bird and Dorn (1968) who concluded that in the regime of high temperatures ( $>0.5 T_m$ ) and intermediate stresses where dislocation processes are likely to dominate deformation behavior, the best description of creep is given by an expression of the form

$$\dot{\epsilon} = A \frac{Gb}{kT} \left(\frac{\sigma}{G}\right)^n D \quad (1)$$

where  $\dot{\epsilon}$  is the steady-state creep rate,  $G$  is the shear modulus,  $b$  is the Burgers vector,  $k$  is the Boltzmann constant,  $T$  is the absolute temperature,  $\sigma$  is the applied stress,  $D$  is the diffusivity, and  $A$  and  $n$  are dimensionless constants. The diffusivity term  $D$ , being of the form

$$D = D_0 e^{-Q_c/RT}, \quad (2)$$

contains the temperature dependence of the creep rate; the activation

energy for creep  $Q_c$  has been shown to accurately agree with the activation energy for self diffusion when the temperature dependence of the shear modulus  $G$  is taken into account in eqn. (1).

Many workers approximate the relationship between creep rate, stress and temperature by a phenomenological expression of the form

$$\dot{\epsilon} = A' \sigma^n e^{-Q/RT} \quad (3)$$

which, as shown by Mukherjee et al. (1968) is neither dimensionally nor experimentally correct unless  $G$  is considered to be temperature independent and incorporated into the constant  $A'$ . Nevertheless, the values of  $n$  are frequently presented as evidence that a particular mechanism is the rate controlling step for creep. In many cases, agreement between directly measured  $Q$  values according to eqn. (3) and self-diffusion activation energies are satisfactory; however, Mukherjee et al. (1968) have shown that in metallic systems the agreement is improved when  $Q_c$  is calculated in terms of the parameters of eqn. (1). The latter procedure also facilitates comparison of the behavior of metallic and non-metallic materials.

The majority of creep measurements reported in the literature on ionic solids have been made on NaCl. The single crystal compression measurements of Christy (1956), Geguzin et al. (1964), Ilschner and Reppich (1963), Blum and Ilschner (1967), and Schuh, Blum and Ilschner (1970) all result in a power law stress dependence of the steady state strain rate with  $n \sim 4-5$ . Activation energy values are not as consistent with a reported range from  $\sim 46$  kcal/mole to  $\sim 82.4$  kcal/mole. In fine-

grained NaCl polycrystals, tested in bending, Kingery and Montrone (1965) observed "viscous deformation" at high temperatures, i.e., strain rate directly proportional to stress and to the diffusivity of the  $\text{Cl}^-$  ion. In contrast, Burke (1968) found a power law relationship for coarse-grained NaCl deformed in compression with a stress exponent of  $n = 5.0$  with an activation energy value of 49 kcal/mole at high temperatures in good agreement with that for  $\text{Cl}^-$  ion lattice diffusion in NaCl. LeComte (1965) measured activation energies for creep in polycrystalline NaCl in compression and found an increase in  $Q$  with temperature from 12.5 kcal/mole at 29°C to 30 kcal/mole at 300°C.

Recently Cannon and Sherby (1970) conducted creep studies in compression on polycrystalline NaCl-KCl solid solutions and found the steady-state creep rate to be proportional to the third power of the stress and to the diffusion coefficient of the cation. Pure polycrystalline KCl was found to obey an  $n = 5$  power law. Other studies on creep behavior in ionic materials include the early work of Christy (1964) on AgBr single crystals in which a  $Q$  somewhat higher than self-diffusion activation energies for either ionic species was measured.

Polycrystalline LiF has been studied under compressive creep conditions by Cropper and Langdon (1968) who found a power law stress dependence with  $n = 6.6$  and an activation energy of 50.1 kcal/mole in good agreement with that for  $\text{F}^-$  diffusion in the intrinsic range. A study of the correlation between activation energies for creep, fracture and sublimation by Betekhtin and Bakhtiboev (1970) was made from creep measurements on NaCl, KCl and LiF single crystals. They concluded that the stress dependence of the steady-state strain rate was logarithmic, i.e.,

$\dot{\epsilon} \propto \sigma^{B\sigma}$  and obtained an activation energy value of  $\sim 70$  kcal/mole for LiF. Studies of high temperature sigmoidal creep in LiF single crystals at low stresses and high temperatures have been reported by Coghlan et al. (1971) and by Menezes and Nix (1971). Rao and Ruoff (1972) studied creep of  $\langle 001 \rangle$  oriented LiF single crystals in the steady state region in the temperature range of  $650-750^\circ\text{C}$  and found stress exponents of 5.1 to 3.7 and an activation energy for creep of 48 kcal/mole.

The purpose of the present investigation is to expand creep measurements on LiF single crystals at high temperatures for crystals in several orientations. An attempt is made to deduce the particular rate controlling mechanism for creep in the limited range of temperatures and stresses considered and the results are compared to those obtained under similar conditions for metals.

## 2. EXPERIMENTAL PROCEDURE

### A. Materials

Lithium fluoride single crystals were purchased from the Harshaw Chemical Company, (Cleveland, Ohio) as cleaved blanks nominally 1 inch by 1 inch by  $1/4$  to  $5/16$  inch thick. Three different commercial grades were obtained, henceforth to be referred to as monochromator quality (Mono.), infra-red quality (I.R.), and vacuum ultra-violet quality (U.V.), in increasing degree of purity. Spectrographic analysis was employed to identify the principal cation impurities present, summarized in Table I. Detection limits are indicated by the numbers in parentheses following each element. From these results, the major difference between the three grades of material appears to be the presence of 300 ppm Mg in the monochromator quality crystals.

Specimens for creep tests were prepared by sawing with a small resin bonded diamond impregnated blade. Crystals to be deformed with the applied stress parallel to  $\langle 100 \rangle$  were obtained by making cuts parallel to the  $\{100\}$  cleavage faces of the blanks. These specimens, henceforth referred to as  $\langle 100 \rangle$  crystals, were right rectangular parallelepipeds normally  $7/16$  to  $1/2$  inch long and  $1/4$  to  $5/16$  inch thick. Length to thickness ratios thus ranged from 1.5 to 2.0. A limited number of  $\langle 100 \rangle$  specimens were prepared in the form of cubes, i.e., with length to thickness ratios of  $\sim 1.0$ .

Crystals to be deformed with the applied stress parallel to  $\langle 111 \rangle$  were cut from cubes of  $\langle 100 \rangle$  oriented crystals using a procedure similar to that described previously for MgO by Hulse et al. (1963). A  $\langle 100 \rangle$  cube was cemented to a jig machined from bakelite such that the  $\langle 111 \rangle$  axis of the cube was parallel to the diamond saw blade. Two identical resin bonded blades separated by a spacer were then employed to make two pairs of parallel cuts at right angles resulting in a prism with square cross-section and a  $\langle 111 \rangle$  axis. Due to the limitation of a  $5/16$  inch maximum thickness of the original cubes, the  $\langle 111 \rangle$  specimens were necessarily smaller than the  $\langle 100 \rangle$  crystals; typical cross sections were  $\sim .140$  inch thick. These crystals were then cut to the appropriate length to obtain length to thickness ratios between 1.5 and 2.0.

After cutting to the appropriate dimensions, all specimens were mounted in a special jig and sanded on both ends with "0" grade emery polishing paper to insure that the ends were flat, parallel to each other and perpendicular to the loading axis. Prior to testing, each crystal was polished for  $1/2$  hour in 85%  $H_3PO_4$  at  $100-120^\circ C$  to remove the surface

damage incurred in cutting. Masking lacquer was used to protect the ends of the specimens from attack during the chemical polish in order to maintain flatness. Disappearance of birefringence effects from the crystals after chemical polishing confirmed the removal of the damaged surface layer.

#### B. Apparatus

Specimens were tested in compression in a small dead-load testing machine similar to that described by Sherby (1958). The total strain was continuously measured by a linear variable differential transformer and recorded by a recording potentiometer. Overall strain sensitivity was  $\pm 5 \times 10^{-5}$ . Elevated temperatures were obtained by a small resistance furnace positioned around the specimen and were constant to within  $\pm 1^\circ\text{C}$  of the reported values.

#### C. Creep Tests

Specimens were placed between two 99.5%  $\text{Al}_2\text{O}_3$  buttons for creep testing to protect them from contact with the stainless steel loading platens. A 0.0005 inch thick platinum foil between the LiF crystal and the  $\text{Al}_2\text{O}_3$  buttons acted as a lubricant and allowed the crystal ends to spread during the course of a test, thus essentially eliminating barreling which frequently occurs in specimens tested in compression. Those portions of the Pt foil extending outward from beneath the LiF crystals were observed to undergo some chemical attack, particularly after tests at higher temperatures and longer times. A yellow-green powdery residue was often observed around the edges of the crystal while the crystal itself remained colorless and apparently free from contamination. The major portion of the Pt foil between the LiF crystal and the  $\text{Al}_2\text{O}_3$

button was not attacked. Test temperatures (650°-750°C) were reached after heating for four to six hours, and specimens were normally held at temperature for several hours prior to applying the load.

The majority of the creep tests were performed at a single stress and temperature. To insure that a constant stress was maintained throughout the test, additional predetermined load increments were added at engineering strain intervals of 0.01 to compensate for the increase in cross-section with compressive strain. Initially these increments were calculated by assuming constancy of volume and neglecting any barreling that may have occurred. Subsequently, as the number of crystals tested increased, it was possible to develop an empirical correction based on the actual change in cross-section as a function of strain. Thus the maintenance of a true constant stress level throughout the course of a test was assured.

A small number of crystals were subjected to "incremental" creep tests, i.e., tested at a constant temperature and a number of different stresses or alternatively deformed under a constant stress while the temperature was cycled over a narrow range. This approach attempts to minimize experimental scatter between specimens for the evaluation of stress and temperature dependence of the creep rate.

#### D. Microstructural Observations

After deformation, specimens were prepared for microstructural observations by sectioning with a resin bonded diamond blade. The crystals were mounted in plastic and polished through "4-0" emery polishing paper followed by polishing with Linde A in water. A chemical polish in a 2% solution of  $\text{NH}_4\text{OH}$  in distilled water at room temperature was used

to remove the surface layers containing damage from the mechanical polishing. Finally, the crystals were etched in a solution of 4%  $\text{HBF}_4$  in 200 proof ethyl alcohol which was shown by Scott and Pask (1963) to reveal dislocations on all crystallographic faces of LiF.

Several back-reflection Laue X-ray patterns were made from deformed crystals to determine a qualitative indication of the degree of polygonization. Specimens were exposed to tungsten  $K_\alpha$  radiation at 50 kV and 20 ma for approximately 20 min.

### 3. RESULTS

#### A. Creep Curves

Several representative creep curves are shown in fig. 1 for I.R. crystals tested at  $700^\circ\text{C}$  in both  $\langle 100 \rangle$  and  $\langle 111 \rangle$  orientations. The principal feature to be noted is the extreme difference in length of primary creep periods for the two different stress axes. The  $\langle 100 \rangle$  crystals exhibited an extraordinarily long primary period; generally true strains as high as 0.20 or greater were required before steady-state creep was established. All crystals tested in the  $\langle 100 \rangle$  orientation exhibited this "exaggerated" primary creep behavior the length of which increased at the higher stresses and temperatures.

Crystals tested in the  $\langle 111 \rangle$  orientation, on the other hand, exhibited short primary creep periods, as little as 0.02-0.05 true strain being required for the establishment of steady-state conditions. Despite the large differences in primary creep periods, the final steady-state strain rates for crystals in the two orientations tested at a given stress were normally within a factor of two of each other although the  $\langle 100 \rangle$  crystals usually had the higher rate, as shown in fig. 1. The

figure also indicates that the time to reach equivalent strains is much longer for the  $\langle 111 \rangle$  orientation.

#### B. Stress Dependence

A first approximation of the relationship between the applied stress and the steady-state strain rate may be obtained by considering the experimental data in terms of the phenomenological relationships described previously in eqn. (3). Figure 2 is a plot of the steady-state creep rates as a function of applied stress for  $\langle 100 \rangle$  crystals of I.R. quality (open symbols) deformed at  $650^\circ$ ,  $700^\circ$ , and  $750^\circ\text{C}$  ( $0.8-0.9 T_m$ ) and  $\langle 111 \rangle$  crystals deformed at  $700^\circ\text{C}$ . Data for mono-quality and U.V. quality crystals are shown by half shaded symbols while the  $\langle 111 \rangle$  crystals are represented by solid symbols.

The results shown in fig. 2 indicate that the relationship between steady-state strain rate and stress is in the form of a power law with the value of the stress exponent, corresponding to  $n$  in eqn. (3), equal to 3.9 for  $650^\circ$  and  $700^\circ\text{C}$  and 4.0 for  $750^\circ\text{C}$  I.R. quality  $\langle 100 \rangle$  crystals. Slightly lower values of the stress exponent were obtained for Mono. ( $n = 3.6$ ) and U.V. ( $n = 3.9$ ) crystals at  $700^\circ\text{C}$  but since only three points each were obtained for these materials, the difference between them and the I.R. results is not considered to be significant. A power law relationship is also indicated for  $\langle 111 \rangle$  crystals with a calculated value of  $n = 3.4$ . A comparison of the  $\langle 111 \rangle$  data with the data for  $\langle 100 \rangle$  crystals at  $700^\circ\text{C}$  reveals rather close agreement between steady-state strain rates at corresponding stresses. This is particularly noteworthy in light of the marked contrast between the shape of the creep curves for the two orientations and the correspondingly much longer time

for a  $\langle 111 \rangle$  oriented crystal to reach an equivalent strain.

Several  $\langle 100 \rangle$  crystals prepared in the form of cubes ( $l/t = 1.0$ ) were deformed at  $700^\circ\text{C}$  for comparison with crystals of the normal size ( $l/t = 1.5-2.0$ ). These results, indicated by starred (\*) points in fig. 2, were similar to the normal shaped specimens in that the stress exponent calculated from the four data points was equal to 4.1. The general consequence of reducing the aspect-ratio of single crystal creep specimens appears to be a reduction in steady-state strain rate for a given stress without affecting the stress exponent. Langdon and Pask (1970) observed a similar reduction in strain rate with  $l/t$  for polycrystalline MgO creep experiments in compression while the stress exponent remained constant.

### C. Incremental Stress Tests

Crystals tested in the  $\langle 100 \rangle$  orientation gave inconsistent results when attempts were made to ascertain the stress dependence by the incremental technique. That true strains on the order of 0.20 were required before steady-state conditions were established particularly limited the usefulness of this approach for on changing the stress to higher values, new primary creep usually ensued requiring excessive total strains for the completion of the test. Also, strain rates were not reproducible on returning to a given stress after an intermediate stress change.

Contrasted to this unpredictable behavior,  $\langle 111 \rangle$  crystals responded in an entirely consistent and reproducible manner to the incremental technique. For example, the results are shown in fig. 3 for a  $\langle 111 \rangle$  crystal subjected to stresses between 100 psi and 250 psi during a single test sequence at  $700^\circ\text{C}$ . The points plotted correspond to the ratios of

stresses and steady state strain-rates after and before a given change of stress. The slope of the line shown results in a value of  $n = 3.3$  in excellent agreement with the  $n = 3.4$  value obtained for  $\langle 111 \rangle$  crystals in constant stress tests.

#### D. Temperature Dependence

To determine the apparent activation energy for creep, corresponding to  $Q$  in eqn. (3), values of  $\ln \dot{\epsilon}$  were plotted as a function of reciprocal absolute temperature for various constant stress levels. The results are shown in fig. 4. Values for  $Q$  calculated from the slopes of the lines shown range from 64.1 to  $65.6 \pm 7$  kcal/mole suggesting that the apparent activation energy is independent of stress, purity and crystal orientation over the range of experimental conditions considered.

#### E. Incremental Temperature Tests

Crystals tested in the  $\langle 100 \rangle$  orientation exhibited the same difficulties when subjected to incremental temperature tests as described previously for change in stress experiments. It was therefore impossible to determine a reliable value for  $Q$  by this method.

In contrast, the results obtained from incremental tests for  $\langle 111 \rangle$  crystals were, as for the incremental stress experiments, consistent and reproducible. The results are shown in fig. 5 for a  $\langle 111 \rangle$  I.R. quality crystal cycled between  $725^\circ$  and  $750^\circ\text{C}$  at a constant stress of 200 psi. Here, steady-state conditions were established quickly since the crystal responded rapidly to a change in temperature. The values of  $Q$  calculated from each change, averaging 65.7 kcal/mole, were closely grouped and in good agreement with the results from isothermal tests for  $\langle 111 \rangle$  crystals shown in fig. 4, confirming the invariance of apparent

activation energy with crystal orientation.

#### F. Modulus of Elasticity

The recent work of Mukherjee et al. (1968) has shown how the apparent activation energy  $Q$  obtained from direct experimental measurements may be in error due to the effect of the temperature variation of the shear modulus  $G$  on the constant term  $A'$  in eqn. (3). To determine this effect for the present work, eqn. (1) is arranged in the form

$$\frac{\dot{\epsilon}T}{G} = A'' \left(\frac{\sigma}{G}\right)^n e^{-Q_c/RT} \quad (4)$$

where  $A''$  is a new constant incorporating  $b$  and  $k$ . Taking data at a constant value of  $\frac{\sigma}{G}$  and two temperatures  $T_1$  and  $T_2$ , the corrected value of activation energy is given by

$$Q_c = \frac{R \ln \frac{(\dot{\epsilon}T/G)_2}{(\dot{\epsilon}T/G)_1}}{(T_2 - T_1)/T_1 T_2} \quad (5)$$

Shear modulus values for LiF single crystals obtained from the high temperature measurements of Hart (1968), listed in Table II, were used to calculate values of  $\frac{\dot{\epsilon}T}{G}$  and  $\frac{\sigma}{G}$  which were then plotted for  $\langle 100 \rangle$  crystals in fig. 6. For constant values of  $\frac{\sigma}{G}$  between  $7 \times 10^{-5}$  and  $1.5 \times 10^{-4}$  the calculated values of  $Q_c$  ranged from 51.0 kcal/mole to 55.2 kcal/mole, about 10 kcal/mole less than the apparent activation energy values obtained from fig. 4.

## 4. DISCUSSION

A. Shape of Creep Curve

The primary or decreasing strain rate portion of a creep curve is usually associated with the development of a stable substructure characteristic of the experimental conditions. The marked contrast in length of primary creep period for  $\langle 100 \rangle$  and  $\langle 111 \rangle$  oriented crystals, as shown in fig. 1, then probably reflects differences in the processes controlling the generation of substructure.

For crystals oriented with the applied stress parallel to  $\langle 100 \rangle$ , four  $\{110\} \langle \bar{1}\bar{1}0 \rangle$  slip systems are equally stressed. The studies of Copley and Pask (1965) and Day and Stokes (1964) on MgO and the more recent work of Day and Johnston (1969) on LiF have demonstrated the increasing resistance to dislocation intersections on orthogonal and oblique  $\{110\}$  slip planes. For LiF crystals pulled in tension at initial strain rates of  $\sim 8 \times 10^{-4} \text{ sec}^{-1}$ , Day and Johnston (1969) have shown that even at  $700^\circ\text{C}$  ( $0.87 T_m$ ) interpenetration of slip on orthogonal systems did not occur freely and that oblique slip was even more difficult. Orthogonal intersections should result in formation of jogs as the two intersecting dislocations cannot lower their energy by combining to form a third dislocation. Dislocations intersecting on oblique  $\{110\}$  planes can react to form a third sessile dislocation lying parallel to  $\langle 111 \rangle$ . Arrays of these pure edge sessile dislocations are thought to restrict themselves by climb processes at temperatures above  $0.5 T_m$ . That low strains in excess of 0.20 are required for the establishment of steady state creep in  $\langle 100 \rangle$  crystals may reflect the continuing resistance to intersection and subsequent rearrangement of dislocations moving on

oblique  $\{110\}$  planes.

In contrast to the behavior of  $\langle 100 \rangle$  crystals, dislocations moving on the three equally stressed  $\{100\}$  glide planes for crystals in the  $\langle 111 \rangle$  orientation do not react upon intersection. This may be reflected in the relatively short primary period observed for  $\langle 111 \rangle$  crystals as steady-state conditions are established within a few minutes of the application of the stress and after a small true strain.

#### B. Stress Dependence

The value of the stress exponent,  $n$ , in eqn. (3) may be used as an indication of the particular rate controlling mechanism for creep. For polycrystalline materials under conditions where creep occurs without the motion or interaction of dislocations, so-called "viscous" or diffusional creep, a stress exponent of 1 is often found as predicted by the theories of Nabarro (1948), Herring (1950), and Coble (1963). Creep models involving the motion of dislocations either by glide or climb predict higher values of  $n$ . In a recent review of dislocation models of creep, Weertman (1968) has shown how  $n$  may be found to vary from 3 to 6 or even higher, depending on the particular dislocation mechanism predominating.

Over the limited range of stresses and temperatures employed in this investigation, experimental values of  $n$  range from 3.6 to 4.1 for  $\langle 100 \rangle$  oriented crystals of all purities, and equal 3.4 for  $\langle 111 \rangle$  oriented I.R. quality crystals. The observed values of  $n$  thus fall within the range anticipated for a rate controlling mechanism involving climb or other non-conservative motion of dislocations.

The various theoretical models of creep deformation were recently reviewed by Mukherjee, Bird and Dorn (1968) who concluded that for metals exhibiting a stress exponent in the range from 3 to 6, the climb of edge dislocations is the most probable rate controlling mechanism for creep. The dislocation climb theories of Weertmann (1957), Chang (1963) and Nabarro (1967) predict a power-law stress dependence with  $n = 4.5$ ,  $4.0$  and  $3.0$  respectively, all in agreement with the range of experimentally observed values. Gifkins (1970) has pointed out the dangers in attempting to unambiguously identify creep mechanisms from measurements made over limited ranges of the experimental variables. Therefore, on the basis of relative agreement of the measured and anticipated values of  $n$ , a dislocation climb mechanism of some type is thought to control the high temperature creep behavior of LiF single crystals.

### C. Temperature Dependence

The activation energies for creep deformation in many materials have been shown to agree well with activation energies for self diffusion. For pure metals with but one atomic species the agreement is particularly good while in non-metallic systems there are not yet sufficiently numerous or precise measurements to reach the same conclusion with complete certainty.

Table III summarizes the activation energies for diffusion in lithium fluoride obtained from NMR measurements by Eisenstadt (1963) and Stoebe and Huggins (1966) and from the conductivity data of Haven (1950). Experimental values of  $Q$  from isothermal tests for  $\langle 100 \rangle$  and  $\langle 111 \rangle$  crystals (fig. 4), averaging 65 kcal/mole, are somewhat in excess of any of the previously reported values for diffusion in lithium fluoride.

However, when the creep equation is correctly formulated to include the effect of temperature variation of the shear modulus, the calculated values of  $Q_c$ , 51-55 kcal/mole, are in good agreement with Eisenstadt's (1963) value for fluorine ion diffusion. This figure also agrees with the results of Cropper and Langdon (1968) for polycrystalline LiF in which the activation energy for creep was determined to be 50.1 kcal/mole. Thus, as in the case for many metallic systems, it appears that the high temperature creep deformation of LiF single crystals is controlled by lattice diffusion with the rate-controlling species being the larger, slower moving fluorine ion.

#### D. Mechanism and Correlation with Other Systems

Following the analysis presented by Mukherjee et al. (1968), a comparison of the data can be made with creep studies in metallic systems by preparing a plot of  $\frac{\dot{\epsilon}kT}{DGb}$  vs  $\frac{\sigma}{G}$ , from eqn. (1), where  $D$  is taken to be the diffusivity of the rate controlling species. Using  $D$  values obtained from the results of Eisenstadt (1963) for  $F^-$  ion diffusion in LiF, and taking  $b = 2.83 \times 10^{-8}$  cm, the data for crystals of both orientations and all purities are shown in fig. 7. The data points for the <100> I.R. quality material at all temperatures and stresses (unshaded symbols) are reduced to a straight line relationship whose slope,  $n$ , is equal to 4.1; the results are thus best represented by the relationship

$$\frac{\dot{\epsilon}kT}{DGb} = 8.9 \times 10^3 \left(\frac{\sigma}{G}\right)^{4.1} \quad (6)$$

The U.V. quality points are superimposed on the pattern of the I.R. data

while the Mono. quality data gives a value of  $n$  of 3.9. The  $\langle 111 \rangle$  data reduces to a straight line relationship with a value of  $n$  of 3.1; the displacement of the line relative to that for the  $\langle 100 \rangle$  data is due to the difference in the shear modulus  $G$  for the two orientations (Table II). The displacement of the line for the Mono. quality  $\langle 100 \rangle$  data relative to the I.R. and U.V. quality  $\langle 100 \rangle$  data is due to lower strain rates for equivalent test conditions because of a higher magnesium content (Table I).

These results for single crystal LiF agree well with the general findings of Mukherjee et al. (1968) for f.c.c. metals which are represented by the area between the two dashed lines. In addition, the data obtained by Cropper and Langdon (1968) for polycrystalline LiF, when plotted in terms of the dimensionless parameters of fig. (7) very nearly coincide with the  $\langle 100 \rangle$  oriented single crystal results. The stress exponent found in that study was considerably higher than that observed here ( $n = 6.6$  vs  $n = 4.1$ ), and may reflect the additional constraint imposed on the deformation process by the presence of grain boundaries. Nevertheless, the agreement between results for single crystal and polycrystalline LiF with the general trends observed in f.c.c. metal leads to the general conclusion that similar mechanisms, probably involving the climb of dislocations, control the high temperature creep behavior of these materials.

#### E. Microstructure

Back reflection Laue X-ray photographs of  $\langle 100 \rangle$  oriented crystals indicated extensive subgrain formation by the replacement of each of the single spots in the pattern of the undeformed crystal with an array of spots each diffracted from a different slightly misoriented subgrain in the deformed crystals. On the basis of the Laue patterns, the degree of misorientation between subgrains is estimated to be not more than about five degrees.

Optical microscopy confirmed the formation of subgrains which were revealed by sectioning the deformed crystals parallel to the stress axis, chemically polishing and etching the surface. A particularly clear example of how the creep substructure may develop from slip bands introduced early in the deformation process is provided in fig. 8, a photomicrograph taken near the end of a  $\langle 100 \rangle$  crystal deformed at  $650^\circ\text{C}$  and 200 psi. This structure suggests that  $\{110\}$  slip bands may provide the framework for subgrain boundaries which develop here predominantly at angles of  $45^\circ$  to the stress axis (horizontal).

The relationship between observed subgrain diameter and applied stress is apparently similar to that observed for metals in that the subgrain size decreases with increasing stress. Using the linear intercept method, estimates of the subgrain diameter  $\delta$  at various stress levels were obtained from  $\langle 100 \rangle$  and  $\langle 111 \rangle$  crystals deformed at  $700^\circ\text{C}$  and are plotted as dimensionless ratios  $\delta/b$ , where  $b$  is the Burgers vector, vs the dimensionless stress function  $\frac{\sigma}{G}$  in fig. 9. The calculated slopes of the lines through the data points are  $-0.93$  for  $\langle 100 \rangle$  and  $-1.2$  for  $\langle 111 \rangle$  crystals, which are in good agreement with the experimental observation for metals that subgrain diameter is proportional to the  $-1$  power of the applied stress.

That well defined subgrains do form during creep of LiF single-crystals is yet another piece of evidence that creep in this system is controlled by a dislocation climb mechanism.

## 5. CONCLUSIONS

1. The creep deformation of LiF single crystals is characterized by extended primary creep for crystals in  $\langle 100 \rangle$  orientation with strains of 0.20 or more required for the establishment of steady-state creep. In contrast, crystals deformed in  $\langle 111 \rangle$  orientation reach steady-state conditions rapidly with primary creep strains of 0.05 or less required. Despite the difference in primary creep behavior for the two orientations, steady-state creep rates at corresponding stresses and temperatures are within a factor of two, with  $\langle 100 \rangle$  crystals having the higher rate.

2. The stress dependence of the steady-state creep rate was determined to be in the form of a power law for crystals of both  $\langle 100 \rangle$  and  $\langle 111 \rangle$  orientations, and impurity concentrations up to 300 ppm, with the stress exponent  $n$  ranging from 3.1 for  $\langle 111 \rangle$  crystals to 4.1 for  $\langle 100 \rangle$  crystals. The effect of reducing the initial length/thickness ratios of the specimens from the normal 1.5-2.0 to cube proportions ( $l/t = 1.0$ ) appears to be a uniform decrease in steady-state strain rate without changing the stress exponent.

3. The activation energy for creep was determined to be  $53 \pm 7$  kcal/mole over the temperature range considered, regardless of crystal orientation or purity. This compares favorably with the activation energy for lattice diffusion of the fluorine ion in LiF, 50.7 kcal/mole.

4. Attempts to determine the stress exponent and activation energy by the incremental technique were unsuccessful for  $\langle 100 \rangle$  crystals. The structural changes accompanying the long primary creep period apparently contribute to the large amount of scatter and non-reproducibility observed for that orientation. In contrast  $\langle 111 \rangle$  crystals responded

to the incremental technique and gave results in good agreement with values for  $n$  and  $Q_c$  obtained from isothermal and constant stress tests.

4. Well developed subgrains were observed in both  $\langle 100 \rangle$  and  $\langle 111 \rangle$  crystals. The subgrain diameter, determined from optical microscopy, was found to vary inversely with the applied stress in agreement with results for many metals.

5. When formulated in terms of the dimensionless parameters  $\frac{\epsilon kT}{DGb}$  and  $\frac{\sigma}{G}$ , the results for LiF single crystals fall in the range observed for metals when creep is dependent upon a dislocation climb process.

The results thus suggest that the creep of LiF single crystals, over the range of experimental variables encountered here, is probably similar to that observed for many metals, and is dependent upon a dislocation climb process.

#### ACKNOWLEDGMENTS

Appreciation is expressed to Professor John Dorn for helpful discussions, to Bill Bullis and Jack Wodei for assistance with the construction of the experimental apparatus, and to John Sherohman for help in running the tests and reducing the data.

This work was supported by the United States Atomic Energy Commission.

## REFERENCES

- BELEKHTIN, V. I., and BAKHTIBAEV, A. N., (1970), *Sov. Phys. Sol. State*, 12, [2], 338.
- BLUM, W., and ILSCHNER, B., (1967), *Phys. Stat. Sol.*, 20 [2], 629.
- BURKE, P. E., (1968), SU-DMS-68-T-59 Ph.D. Thesis, Stanford University.
- CANNON, W. R., and SHERBY, O. D., (1970), *J. Am. Ceram. Soc.*, 53 [6], 346.
- CHANG, R., (1963), The Physics and Chemistry of Ceramics, pp. 275-285, New York, Gordon and Breach.
- CHRISTY, R. W., (1956), *Acta Met.*, 4 [5], 441.
- CHRISTY, R. W., (1964), *Acta Met.*, 2 [3], 284.
- COBLE, R. L., (1963), *J. Appl. Phys.*, 34, [6], 1679.
- COGLAN, W. A., MENEZES, R. A., and NIX, W. D., (1971), *Phil. Mag.*, 23 [186], 1515.
- COPLEY, S. M., and PASK, J. A., (1965), *J. Am. Ceram. Soc.*, 48, [3], 139.
- CROPPER, D. R., and LANGDON, T. G., (1968), *Phil. Mag.*, 18, [156], 1181.
- DAY, R. B., and STOKES, R. J., (1964), *J. Am. Ceram. Soc.*, 47, [10], 493.
- DAY, R. B., and JOHNSTON, W. A., (1969), *J. Am. Ceram. Soc.*, 52, [11], 595.
- EISENSTADT, M., (1963), *Phys. Rev.*, 132, [2], 630.
- GEGUZIN, Ya. E., ROBERTS, V. L., and CHERNYSHAN, A. A. (1964), *Sov. Phys. Sol. State*, 5 [7], 1387.
- GIFKINS, R. C., (1970), *J. Mat. Sci.*, 5, [2], 156.
- HART, S., (1968), *Brit. J. Appl. Phys.*, (J. Phys. D) Ser. 2, 1, [10], 1285.
- HAVEN, Y., (1950), *Rec. Trav. Chim. Pays-Bas*, 69, [11], 1471.
- HERRING, C., (1950), *J. Appl. Phys.*, 21, [5], 437.

- HULSE, C. O., COPLEY, S. M., and PASK, J. A., (1963), J. Am. Ceram. Soc., 46, [7], 317.
- ILSCHNER, B., and REPPICH, B., (1963), Phys. Stat. Sol., 3 [10], 2093.
- KINGERY, W. D., and MONTRONE, E. D., (1965), J. Appl. Phys., 36, [8], 2412.
- LANGDON, T. G., and PASK, J. A., (1970), Acta Met., 18, [5], 505.
- LE COMPTE, P., (1965), J. Geology, 73, [3], 469.
- MENEZES, R. A., and NIX, W. D., (1971), Acta Met., 19, [7], 645.
- MUKHERJEE, A. K., BIRD, J. E., and DORN, J. E., 1968, Lawrence Berkeley Lab. Report UCRL-18526.
- MUKHERJEE, A. K., BIRD, J. E., and DORN, J. E., 1968, Trans. A.S.M., 61, 697.
- NABARRO, F. R. N., (1948), Report of a Conference on Strength of Solids, p. 75, Royal Society, London.
- NABARRO, F. R. N., (1967), Phil. Mag., 16, [140], 231.
- NARAZAN RAO, C. V. S. H., and RUOFF, A. L., (1972), J. Appl. Phys., 43, [4], 1437.
- SCHUH, F., BLUM, W., and ILSCHNER, W., (1970), Proc. Brit. Ceram. Soc., 15, 143.
- SCOTT, W. D., and PASK, J. A., (1963), J. Am. Ceram. Soc., 46, [6], 284.
- SHERBY, O. D., (1958), Trans. Am. Inst. Min. Metal. Engrs., 212, [5], 708.
- STOEBE, T. G., and HUGGINS, R. A., (1966), J. Mat. Sci., 1, [2], 117.
- WEERTMAN, J., (1957), J. Appl. Phys., 28, [3], 362.
- WEERTMAN, J., (1968), Trans. A.S.M., 61, 681.

Table I. Cation impurities in ppm.

Element	Mono.	I.R.	U.V.
Magnesium (5)	300	~5	~5
Calcium (3)	~5	~10	~6
Copper (2)	<2	~2	<2

\* Determined by American Spectrographic Laboratories, Inc., San Francisco, California.

Table II. Shear moduli from direct measurements\*

Temp. (°C)	G<100>		G<111>	
600	1.53 x 10 <sup>11</sup>	$\frac{\text{dynes}}{\text{cm}^2}$ or 2.22 x 10 <sup>6</sup> psi	4.54 x 10 <sup>11</sup>	$\frac{\text{dynes}}{\text{cm}^2}$ or 6.59 x 10 <sup>6</sup> psi
650	1.40 x 10 <sup>11</sup>	"	4.37 x 10 <sup>11</sup>	"
675	1.34 x 10 <sup>11</sup>	"	4.29 x 10 <sup>11</sup>	"
700	1.26 x 10 <sup>11</sup>	"	4.20 x 10 <sup>11</sup>	"
725	1.19 x 10 <sup>11</sup>	"	4.12 x 10 <sup>11</sup>	"
750	1.10 x 10 <sup>11</sup>	"	4.03 x 10 <sup>11</sup>	"

\* Hart (1968)

Table III. Activation energies for diffusion in LiF

Extrinsic		Intrinsic		Ref.
$Q_D(\text{Li}^+)$	$Q_D(\text{F}^-)$	$Q_D(\text{Li}^+)$	$Q_D(\text{F}^-)$	
16.3 kcal/mole	-	41.7 kcal/mole	50.7 kcal/mole	*
15.2	-	43.0	-	**
14.9	-	45.7	-	***

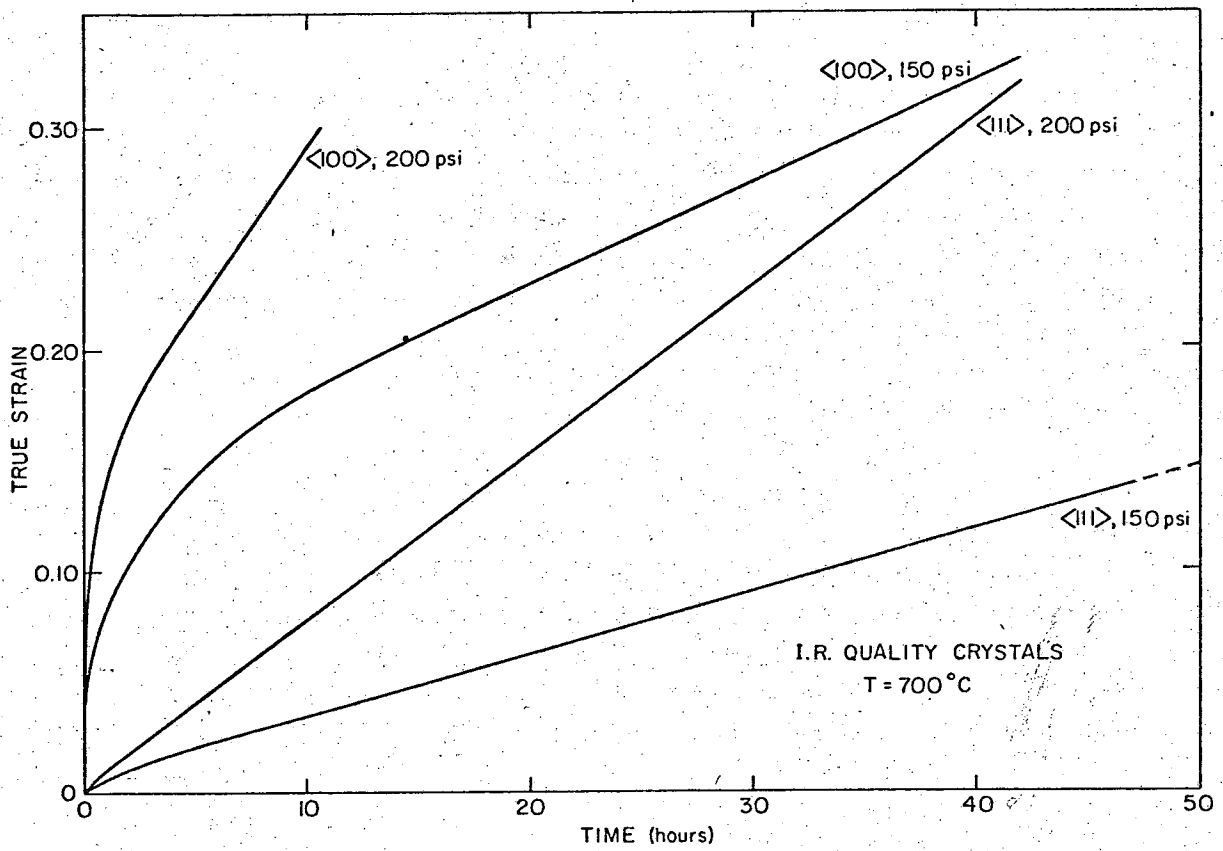
\* Eisenstadt (1963).

\*\* Stoebe and Huggins (1966).

\*\*\* Haven (1950).

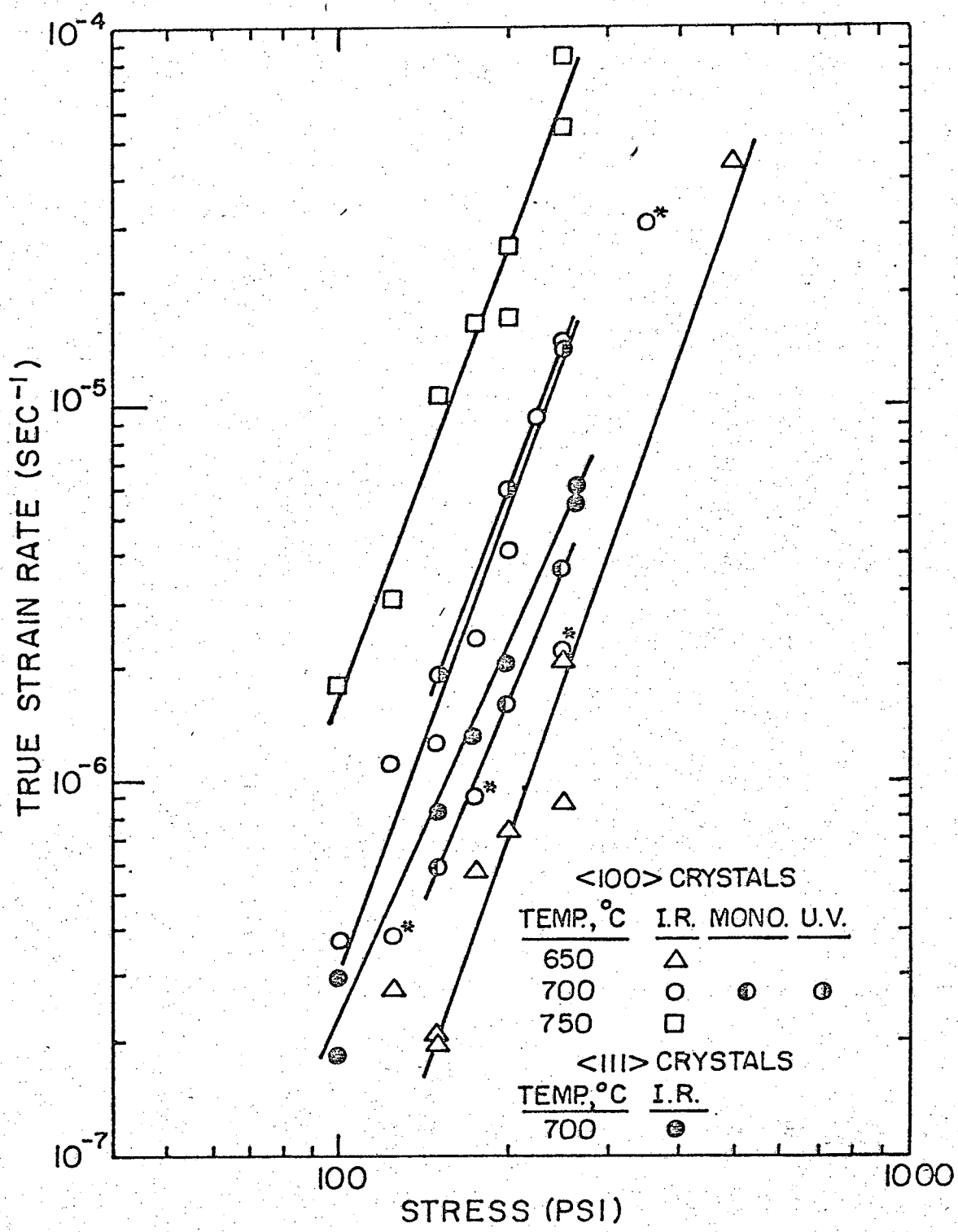
FIGURE CAPTIONS

- Fig. 1. Representative creep curves for  $\langle 100 \rangle$  and  $\langle 111 \rangle$  crystals tested at  $700^\circ\text{C}$  and stresses of 150 and 200 psi.
- Fig. 2. Strain rate vs. stress for  $\langle 100 \rangle$  and  $\langle 111 \rangle$  crystals.
- Fig. 3. Strain rate ratios vs. stress ratios from incremental stress test on a  $\langle 111 \rangle$  crystal at  $700^\circ\text{C}$ .
- Fig. 4. Strain rate vs.  $1/T$  for  $\langle 100 \rangle$  and  $\langle 111 \rangle$  crystals.
- Fig. 5. Strain rate vs. strain for  $\langle 111 \rangle$  crystal in incremental temperature test at a stress of 200 psi.
- Fig. 6. Normalized strain rate vs. normalized stress for  $\langle 100 \rangle$  crystals.
- Fig. 7. Dimensionless strain rate function vs. normalized stress for all crystals.
- Fig. 8.  $\langle 100 \rangle$  crystal deformed at  $650^\circ\text{C}$  and 200 psi.
- Fig. 9. Subgrain diameter vs. normalized stress for  $\langle 100 \rangle$  and  $\langle 111 \rangle$  crystals at  $700^\circ\text{C}$ .



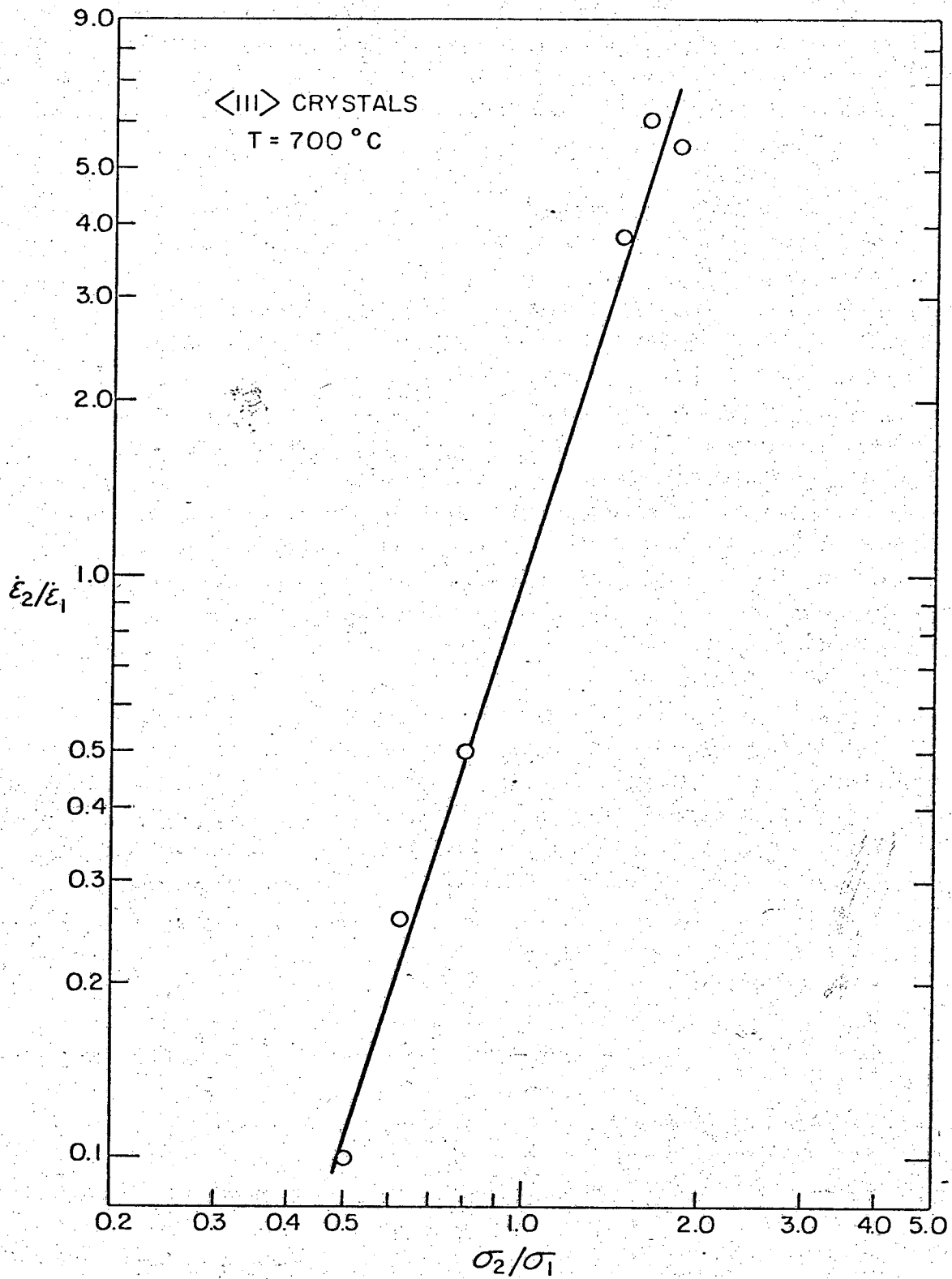
XBL 7012-7232

Fig. 1



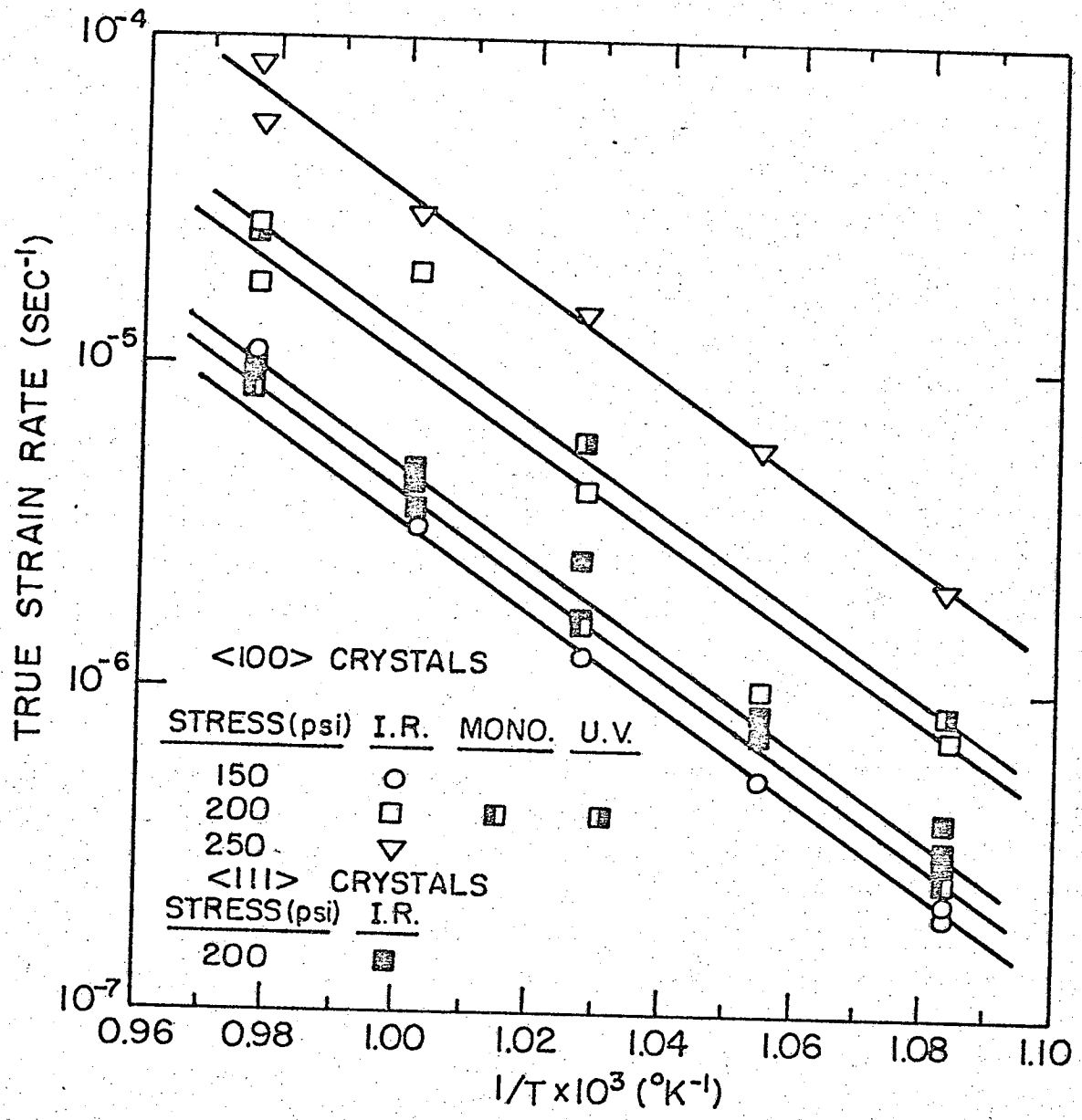
XBL7011-7085A

Fig. 2



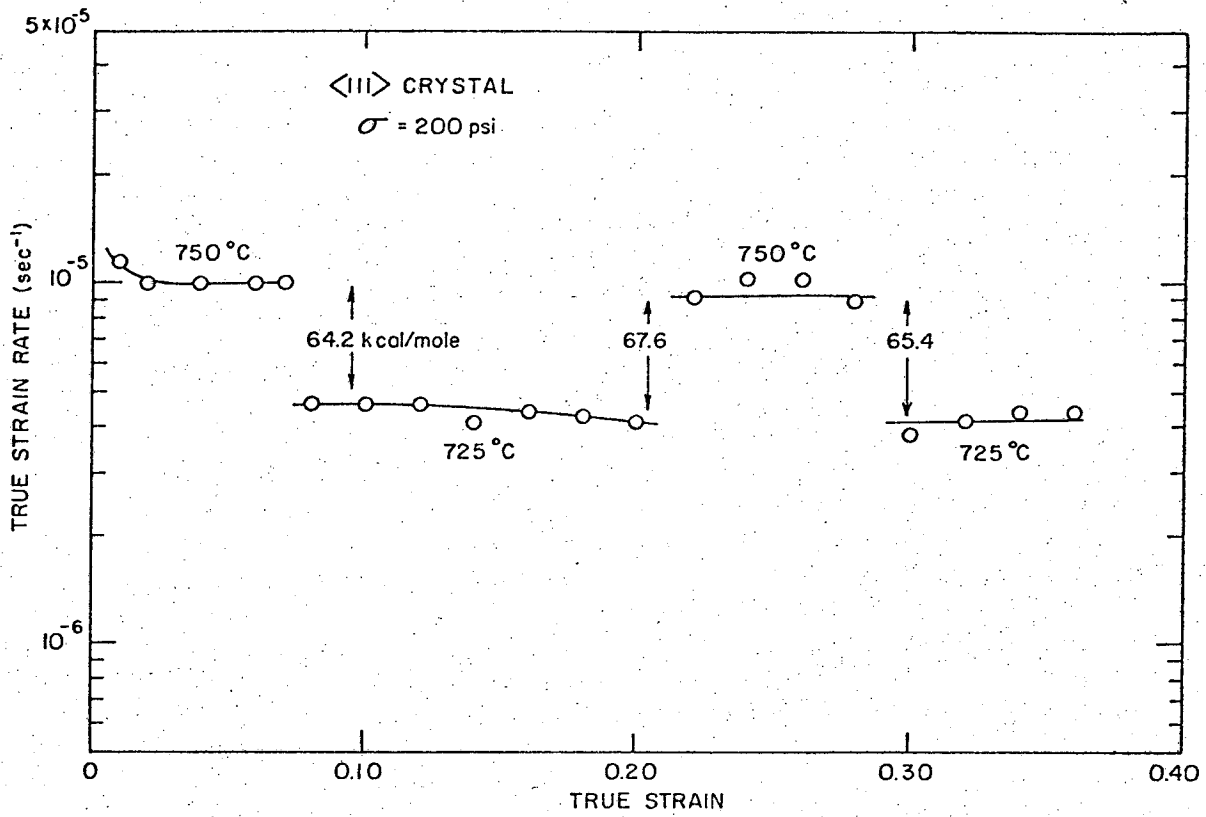
XBL 7012-7224

Fig. 3



XBL 7012-7227A

Fig. 4



XBL 7012-7231

Fig. 5

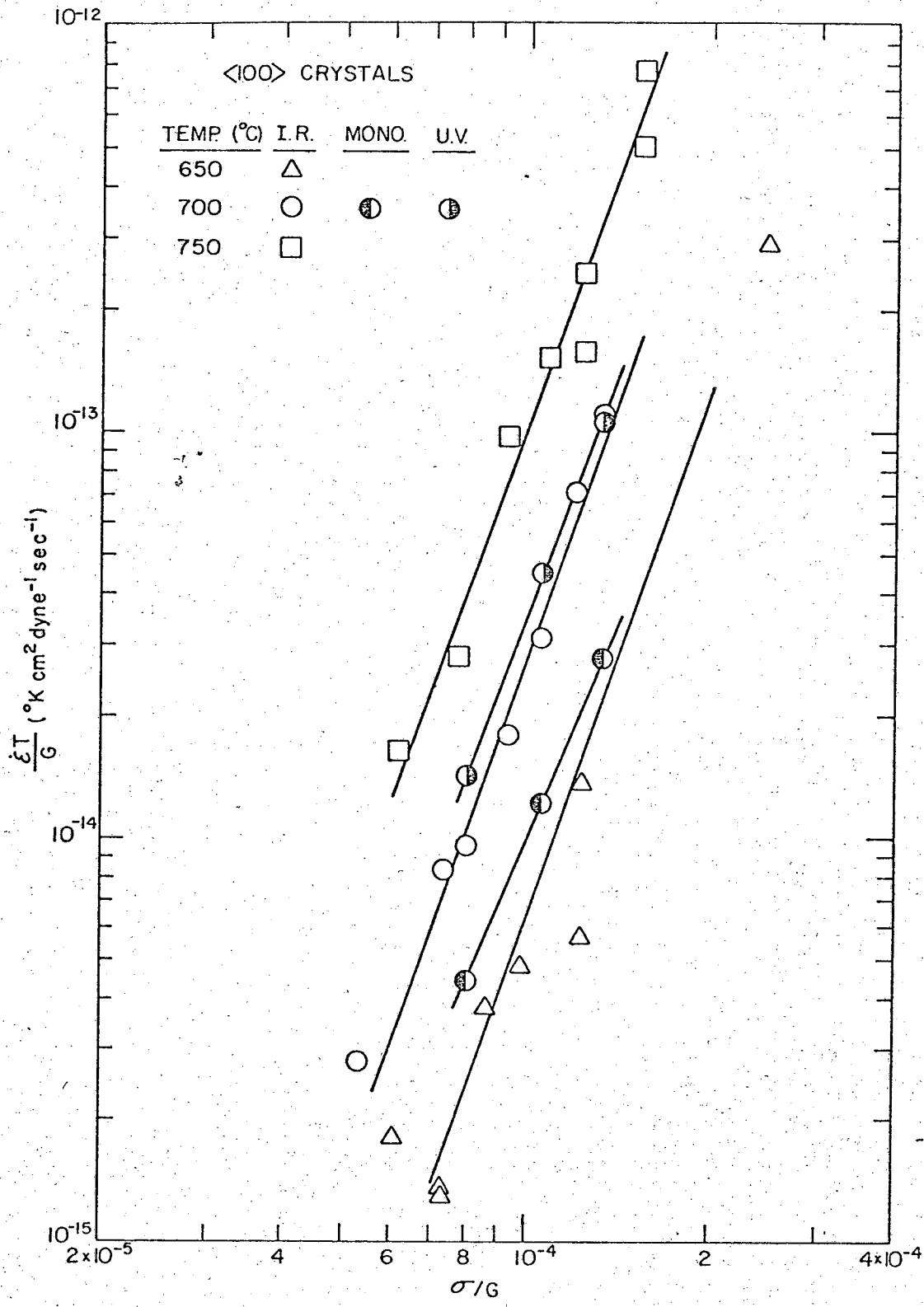


Fig. 6

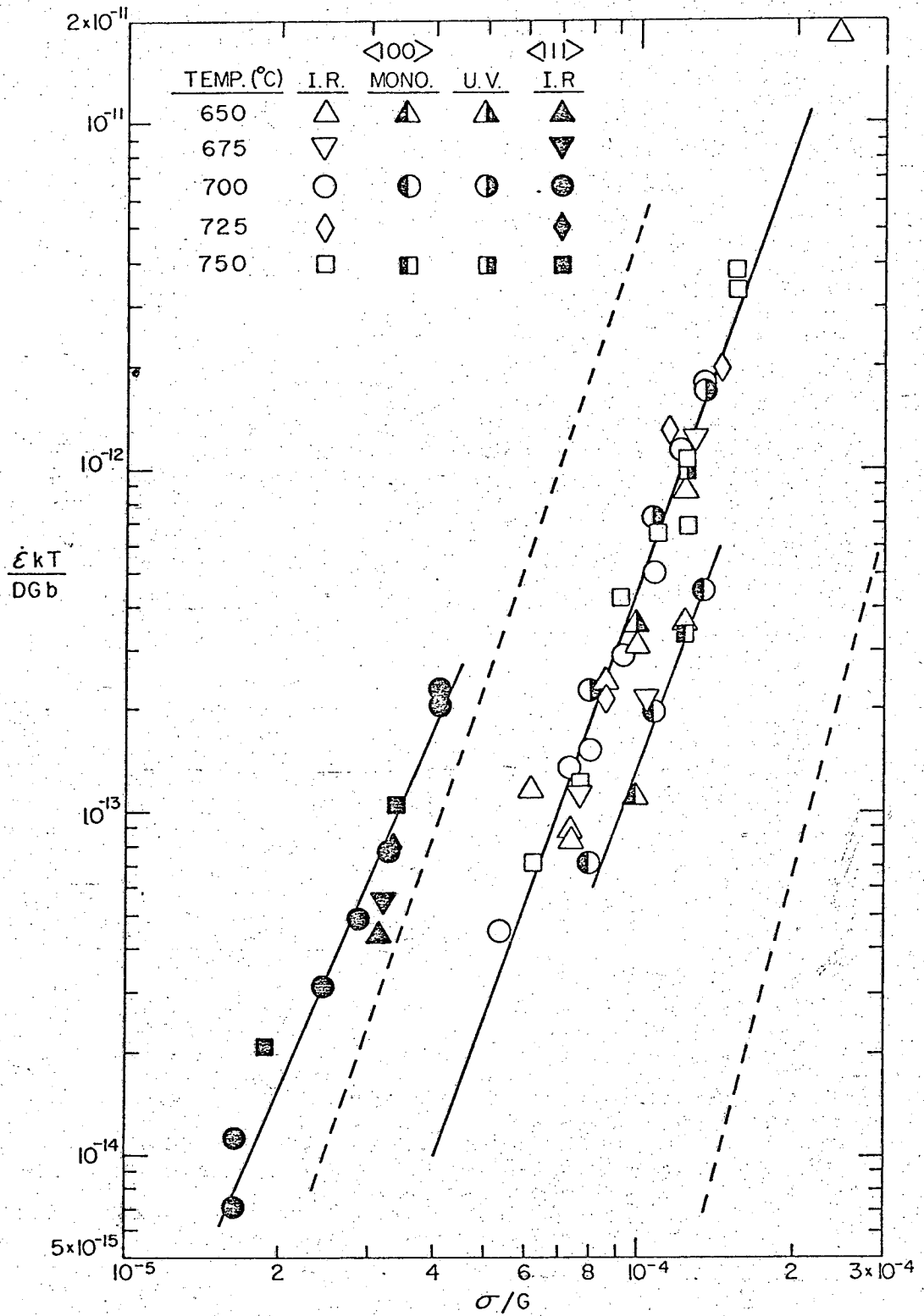
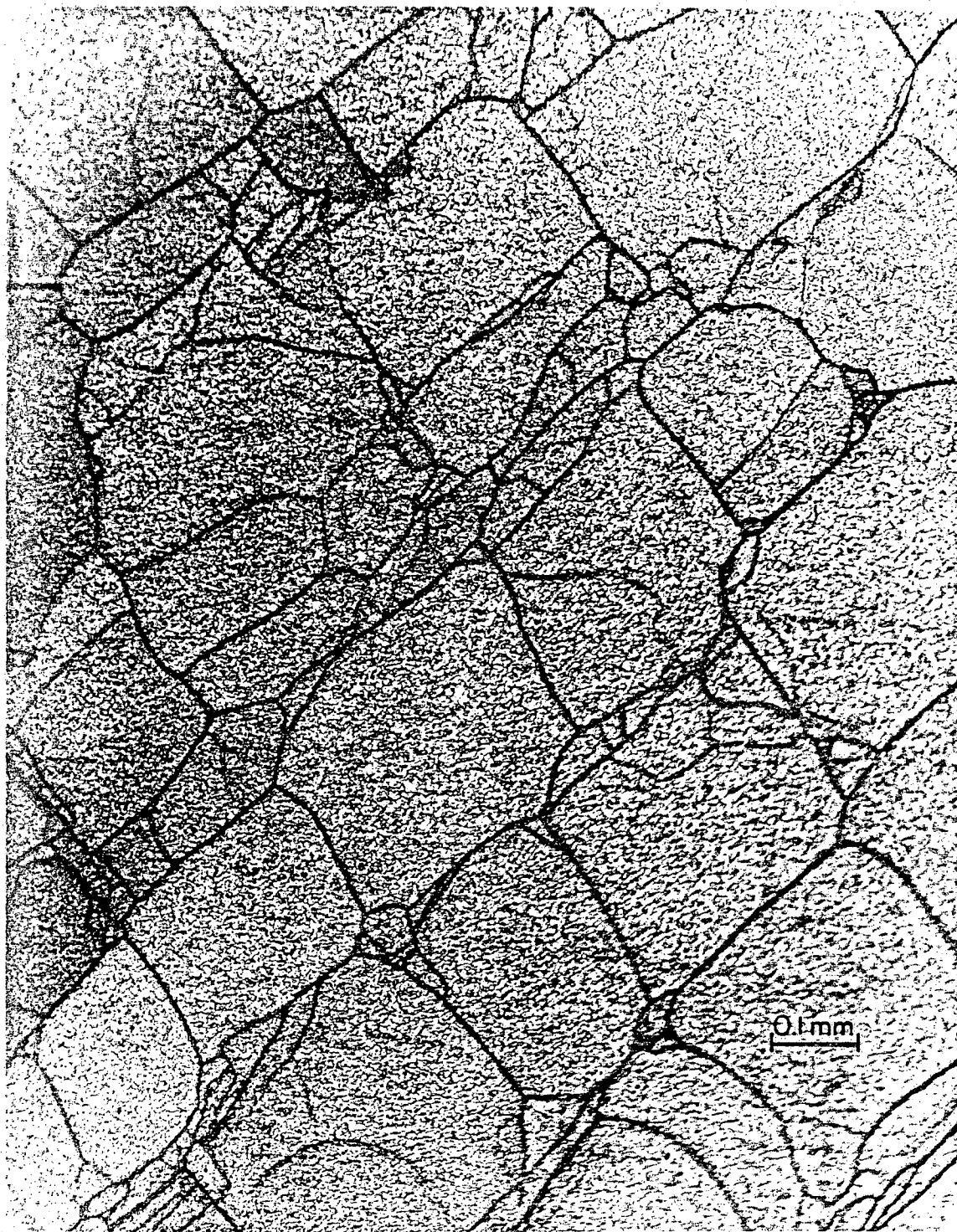
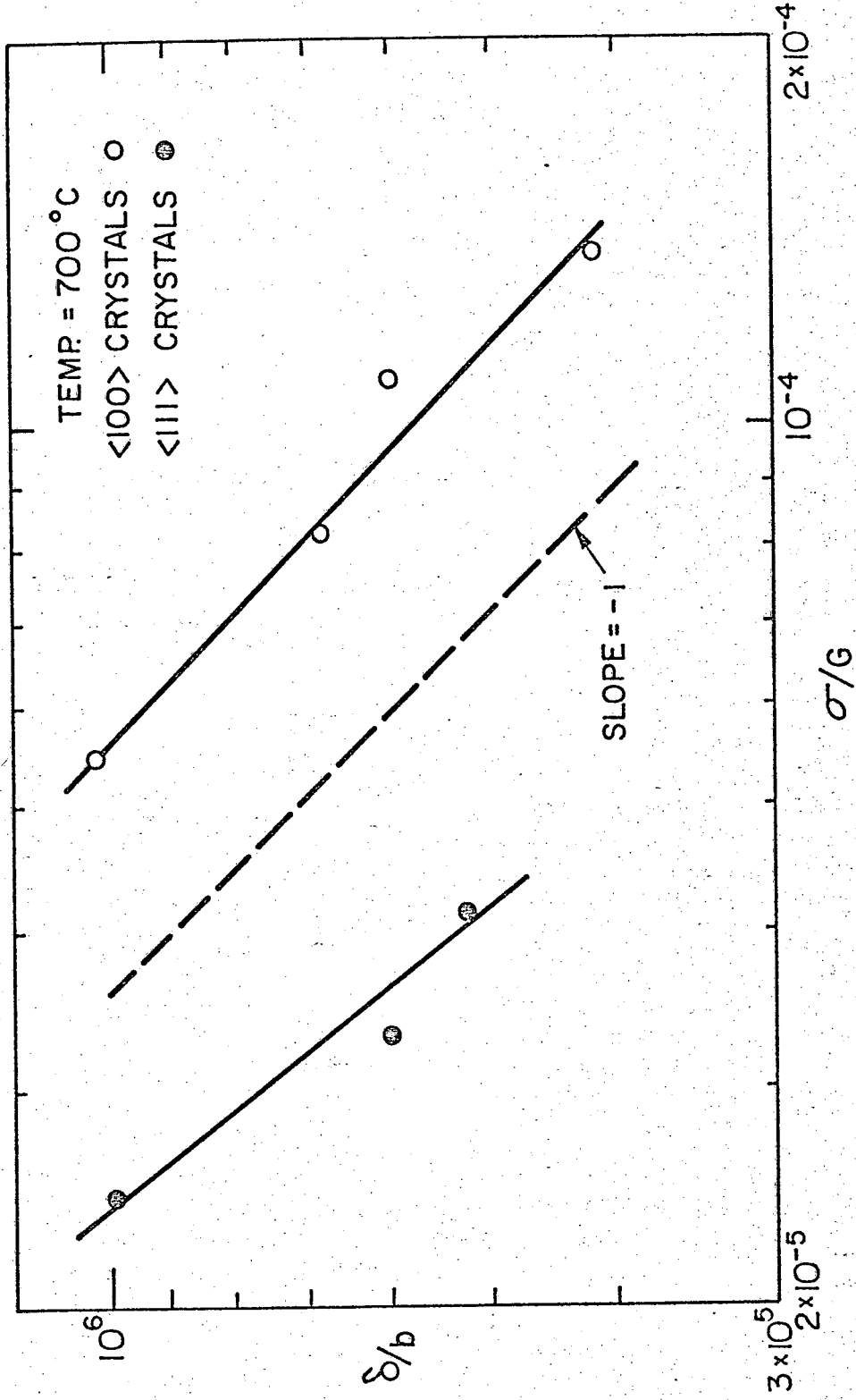


Fig. 7



XBB 7012-5390

Fig. 8



XBL 7012-7225A

Fig. 9

LEGAL NOTICE

*This report was prepared as an account of work sponsored by the United States Government. Neither the United States nor the United States Atomic Energy Commission, nor any of their employees, nor any of their contractors, subcontractors, or their employees, makes any warranty, express or implied, or assumes any legal liability or responsibility for the accuracy, completeness or usefulness of any information, apparatus, product or process disclosed, or represents that its use would not infringe privately owned rights.*

TECHNICAL INFORMATION DIVISION  
LAWRENCE BERKELEY LABORATORY  
UNIVERSITY OF CALIFORNIA  
BERKELEY, CALIFORNIA 94720